A yeast FRET biosensor enlightens cAMP signaling

Dennis Botman[a], Tom G. O'Toole[b], Joachim Goedhart[c], Frank J. Bruggeman[a], Johan H. van Heerden[a], and Bas Teusink[a,*]

[a]Systems Biology Lab/AIMMS, Vrije Universiteit Amsterdam, 1081 HV, Amsterdam, The Netherlands; [b]Department of Molecular Cell Biology and Immunology, Vrije University Medical Center, 1081 HV Amsterdam, The Netherlands; [c]Section of Molecular Cytology, van Leeuwenhoek Centre for Advanced Microscopy, Swammerdam Institute for Life Sciences, University of Amsterdam, 1098 XH Amsterdam, The Netherlands

ABSTRACT **The cAMP-PKA signaling cascade in budding yeast regulates adaptation to changing environments. We developed yEPAC, a FRET-based biosensor for cAMP measurements in yeast. We used this sensor with flow cytometry for high-throughput single cell-level quantification during dynamic changes in response to sudden nutrient transitions. We found that the characteristic cAMP peak differentiates between different carbon source transitions and is rather homogenous among single cells, especially for transitions to glucose. The peaks are mediated by a combination of extracellular sensing and intracellular metabolism. Moreover, the cAMP peak follows the Weber-Fechner law; its height scales with the relative, and not the absolute, change in glucose. Last, our results suggest that the cAMP peak height conveys information about prospective growth rates. In conclusion, our yEPAC-sensor makes possible new avenues for understanding yeast physiology, signaling, and metabolic adaptation.**

Monitoring Editor
Doug Kellogg
University of California, Santa Cruz

Received: May 20, 2020
Revised: Apr 8, 2021
Accepted: Apr 16, 2021

INTRODUCTION

Saccharomyces cerevisiae, or budding yeast, is a unicellular organism that lives in continuously changing environments to which it has to adequately adapt to stay competitive. To do so, yeast cells sense changes in nutrient availability and generate signals that they use as cues to adapt their physiological behavior such as cellular metabolism and growth. For yeast, the most preferred carbon source is glucose, and it has evolved various signaling pathways responsive to its concentration (Rolland *et al.*, 2002; Santangelo, 2006; Rødkaer and Faergeman, 2014). One of these pathways is the cAMP-PKA pathway. Activation of cAMP-PKA occurs when derepressed cells are transitioned to an environment containing an abundant fermentable carbon source. This results in a transient increase of cAMP on a short timescale (i.e., seconds–minutes) and subsequent relaxation to an elevated steady level (Eraso and Gancedo, 1985; Beullens *et al.*, 1988). Activation of the cAMP-PKA pathway occurs via two distinct routes. First, import and metabolism of fermentable sugars activate Ras, stimulated by intracellular acidification (Casperson *et al.*, 1985; Kataoka *et al.*, 1985; Thevelein *et al.*, 1987; Beullens *et al.*, 1988; Mbonyi *et al.*, 1988; Engelberg *et al.*, 1990; Thevelein, 1991; van Aelst *et al.*, 1991; Pardo *et al.*, 1993; Colombo *et al.*, 1998; Rolland *et al.*, 2001). Ras, in turn, activates the adenylate cyclase Cyr1 to produce cAMP. Second, the G–protein-coupled receptor Gpr1 senses extracellular glucose and activates Cyr1 via Gpa2, a G_α protein (Broek *et al.*, 1987; Beullens *et al.*, 1988; Munder and Küntzel, 1989; van Aelst *et al.*, 1990, 1991; Yun *et al.*, 1998; Colombo *et al.*, 1998; Kraakman *et al.*, 1999; Rolland *et al.*, 2000; Lemaire *et al.*, 2004; Kim *et al.*, 2013). Increased cAMP levels lead to activation of PKA by causing dissociation of the regulatory subunit Bcy1 from the PKA subunits (Hixsons and Krebs, 1980; Johnson *et al.*, 1987; Toda *et al.*, 1987). Activated PKA inhibits the stress-related transcription factors Msn2, Msn4, and the Rim15 protein kinase (Martínez-Pastor *et al.*, 1996; Vidan and Mitchell, 1997; Reinders *et al.*, 1998; Smith *et al.*, 1998). Moreover, PKA induces trehalose and glycogen breakdown (van der Plaat, 1974; Hardy *et al.*, 1994; Winderickx *et al.*, 1996) and increases levels of the glycolytic activator fructose-2,6-bisphosphate (Pohlig and Holzer, 1985; Hofmann *et al.*, 1989; Dihazi *et al.*, 2003). Altogether, activation of the cAMP-PKA pathway induces a shift from a slow-growth or stress-resistant physiological state to a fast-growing fermentative one.

This article was published online ahead of print in MBoC in Press (http://www.molbiolcell.org/cgi/doi/10.1091/mbc.E20-05-0319) on April 21, 2021.

Competing interests: The authors declare no competing interests.

*Address correspondence to: Bas Teusink (b.teusink@vu.nl).

Abbreviations used: ConA, Concanavalin A; LP, long pass; PMT, photo multiplier tube; yEPAC, yeast-EPAC; YNB, yeast nitrogen base.

A rise in cAMP is transient, due to its rapid degradation by phosphodiesterase 1 and 2 (Nikawa *et al.*, 1987; Ma *et al.*, 1999; Park *et al.*, 2005). Moreover, the signaling cascade itself is inhibited via feedback inhibition through active PKA (which inhibits various cAMP signaling components). Additionally, cAMP signaling is inhibited by Ira1, Ira2 (which inhibits Ras), and by Rgs2 (which inhibits Gpa2) and these inhibitions also give rise to the transient nature of the response (Nikawa *et al.*, 1987; Tanaka *et al.*, 1989, 1990; Versele *et al.*, 1999; Park *et al.*, 2005; Dong and Bai, 2011; Stewart-Ornstein *et al.*, 2017). A few studies suggest that the glycolytic intermediate fructose-1,6-bisphosphate is an activator of Ras and determines the basal cAMP levels (van Aelst *et al.*, 1991; Colombo *et al.*, 1998; Peeters *et al.*, 2017).

Although much progress has been made on cAMP-PKA signaling in yeast, various questions still remain. For the most part, characterizations were performed using solely glucose (or fructose) as fermentable carbon source. Therefore, cAMP responses to many other carbon sources or to stress-conditions are still largely unexplored. This is mainly because cAMP determination through conventional assay kits is rather labor intensive. Since only a few conditions are generally studied, input-output characterizations of cAMP-PKA signaling are scarce. It is also still unknown whether heterogeneity occurs in single-cell cAMP responses; cell-to-cell heterogeneity is especially relevant for industrial bioprocessing where glucose-signaling heterogeneity can affect industrial efficiency (Altschuler and Wu, 2010; Delvigne *et al.*, 2014; Xiao *et al.*, 2016; Takhaveev and Heinemann, 2018). To address these questions, a cAMP biosensor for yeast would be highly beneficial. The current available cAMP biosensors for yeast (e.g., camp-EPAC2) have a relatively small FRET response and are pH-prone because of the use of pH-sensitive acceptor fluorescent proteins (Bermejo *et al.*, 2013; Colombo *et al.*, 2017; Botman *et al.*, 2019). The latter can especially be an issue since cAMP dynamics are also determined by pH changes as described.

Therefore, we provide an improved genetically encoded biosensor for cAMP. We adapted an EPAC-based FRET sensor originally developed for mammalian cells (Ponsioen *et al.*, 2004; van der Krogt *et al.*, 2008) for use in budding yeast. The resulting yeast-EPAC (yEPAC) sensor contains a FRET pair which is optimal for yeast, measures cAMP with high selectivity, and shows a high FRET ratio change. This enables convenient intracellular measurements of cAMP in living single-yeast cells for the first time. We characterized cAMP responses at the single-cell level and in response to various nutrient transitions. Furthermore, we used flow cytometry to quantify cellular heterogeneity in cAMP dynamics during carbon source transitions. Combined, the obtained cAMP measurements with the new biosensor revealed several novel insights, including a strong dependence of cAMP peak height on the added carbon source and pregrowth conditions. Moreover, the use of yEPAC showed us that, against a fermentative background, the amplitude of the cAMP response (peak height) is a measure for the relative change (i.e., fold change) in glucose concentration, but against a respiratory background, peak height on sugar addition appears to predict the extent of fermentative growth.

RESULTS

Engineering of a versatile EPAC sensor for cAMP quantifications in yeast

In yeast, it is still a challenge to measure cAMP levels continuously in living single cells since a commendable cAMP FRET sensor for yeast is lacking and the current standard of cAMP determination still relies on population-averaged cAMP determination using cell extracts at single timepoints. For mammalian cells, various EPAC-based sensors have been optimized and characterized which provided a good starting point (Ponsioen *et al.*, 2004; van der Krogt *et al.*, 2008; Klarenbeek *et al.*, 2015). These sensors consist of the guanine nucleotide exchange factor Epac1 sandwiched by a fluorescent FRET pair. EPAC1 can bind cAMP which results in a conformational change that can be measured as a change in FRET between the fluorescent FRET pair. From the available sensors, we started with the EPACdDEPCD backbone, which is used in the best performing mammalian-optimized EPAC sensor (Klarenbeek *et al.*, 2015), and replaced the cp173Venus acceptor with tdTomato. This fluorescent protein turned out to be a better acceptor in yeast with proper maturation, a higher photostability, brightness, and pH robustness compared with Venus (Supplemental Figure S1) (Botman *et al.*, 2019, 2020). Furthermore, tdTomato is a good acceptor for mTq2, with a FRET efficiency of 23%, a substantial sensitized emission and no effect of expression levels on FRET ratios (Supplemental Figure S1; Supplemental Table S1), making it very suitable for ratiometric fluorescence readouts. We named this sensor yEPAC.

In vitro calibration of yEPAC showed loss-of-FRET on cAMP addition, and therefore, FRET ratios are presented as CFP/RFP ratios in this paper. We determined that yEPAC has a K_D of 4 μM for cAMP, which is slightly lower compared with the original sensor (Figure 1A) and in the range of physiological cAMP levels in yeast (Russell *et al.*, 1993; Park *et al.*, 2005; Magherini *et al.*, 2006; Xu and Tsurugi, 2006). We performed various control experiments to characterize the performance and potential of yEPAC. We confirmed that glucose addition to cells grown on a nonfermentable carbon source indeed gave a transient cAMP peak up to baseline-normalized FRET values of 1.7 (Figure 1B). We compared yEPAC with the only other available cAMP FRET sensor for yeast (camp-EPAC2) and found a large improvement (maximal response of 1.35 for yEPAC vs. 1.06 for EPAC2). Furthermore, cAMP specificity was confirmed as the $Cyr1^{K1876M}$ mutation in W303-1A and the introduction of the autoinhibiting R279L mutation in the cAMP-binding domain of yEPAC showed a largely diminished cAMP response (Figure 1B) (Vanhalewyn *et al.*, 1999; Ponsioen *et al.*, 2009). The small response of the R279L sensor variant is probably caused by osmotic changes, since the addition of the nonmetabolizable sugar sorbitol gave an identical response of this sensor (Supplemental Figure S1D). Examination of the pH robustness, performed in an in vivo-like manner using the ionophore 2,4-DNP (Thevelein *et al.*, 1987; Botman *et al.*, 2019) and the nonresponding yEPAC-R279L variant, showed robustness between pH 5 and 7.5. We could not use yEPAC since pH also affects cAMP signaling, which would confound the results. Importantly, the yEPAC sensor did not affect growth at various carbon sources (Supplemental Figure S1F). Conversely, however, we did find a small growth rate effect on the FRET levels of the sensor (Supplemental Figure S1G). This makes the sensor less suitable to compare basal cAMP levels at various growth rates. The slight effect of growth rate on basal FRET levels did not affect the actual FRET responses since no relation between the absolute baseline FRET value and the normalized peak height was found ($r = –0.15$, Spearman correlation; Supplemental Figure S1H). The sensor had improved temporal resolution compared with the conventionally used cAMP assay kits since we could record cAMP responses up to 15 min with a 3-s time interval (Figure 1C; Supplemental Movie S1).

yEPAC can also be used in flow cytometry which provides a useful complement to microscopy, as it allows for hundreds to thousands of single cells to be sampled per second. However, this technique cannot measure FRET in the same cells over time. We tested this method with additions of 2 or 100 mM glucose to ethanol-grown cells (Figure 1D). We obtained FRET ratios of 300–700 cells

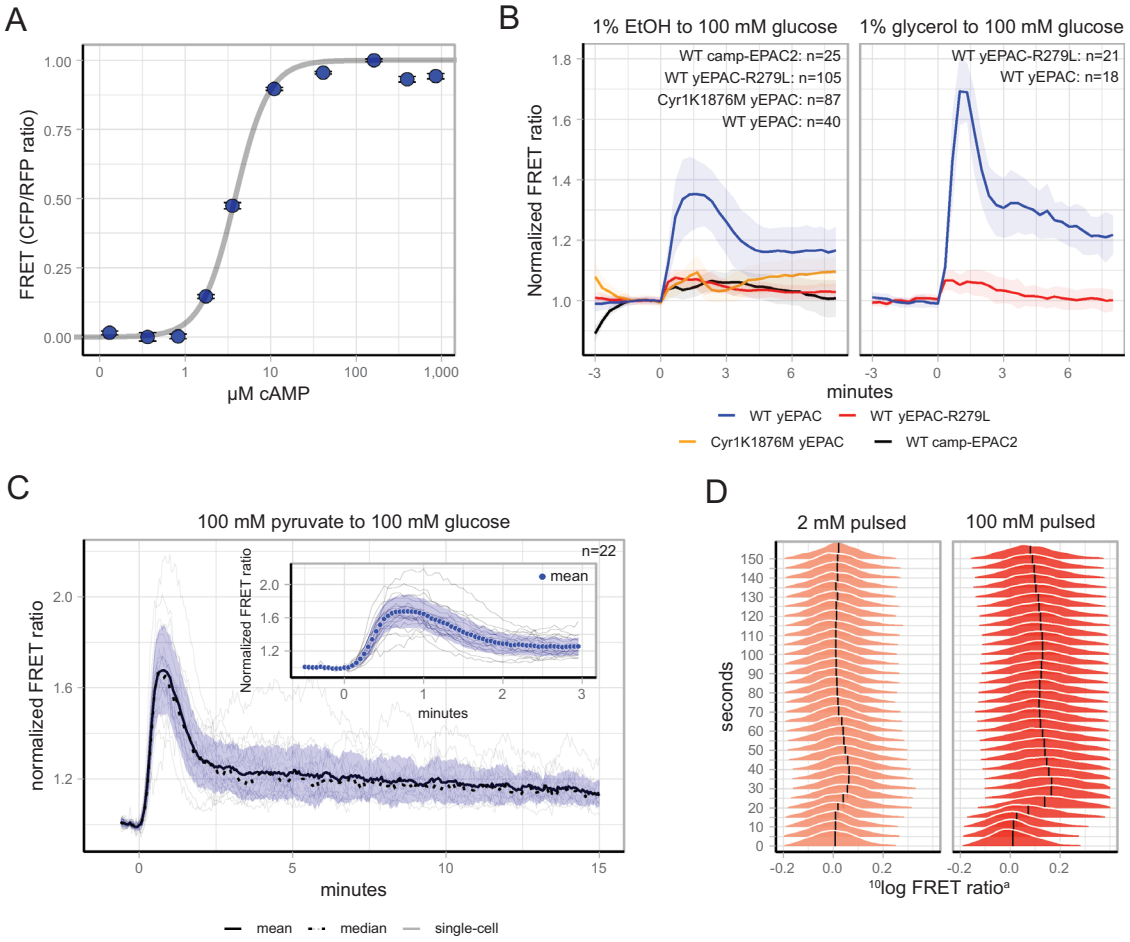

FIGURE 1: yEPAC characterization. (A) In vitro cAMP dose-response curve of yEPAC. Points indicate the mean FRET value of five replicates; error bars indicate SD. Solid line shows the Hill-fit (Eq. 1). (B) W303-1A WT cells expressing yEPAC, the nonresponsive yEPAC-R279L, or camp-EPAC2 and W303-1A cells that possessed the $Cyr1^{K1876M}$ mutation were grown on 1% EtOH or 1% glycerol and pulsed with glucose at $t = 0$ min. FRET signals were obtained and baseline was normalized. Lines show mean FRET ratios; shaded areas indicate SD. (C) Pyruvate-grown W303-1A cells pulsed with 100 mM glucose at $t = 0$ min. Inset shows the first 3 min of the recording. FRET ratios are normalized to the baseline, solid lines show mean FRET ratios, dotted lines show median FRET ratios, gray lines show single-cell trajectories, and shaded areas indicate SD. (D) Dynamic frequency distribution of FRET values after 2 and 100 mM glucose addition, respectively. W303-1A WT cells were pregrown on 1% EtOH, a baseline was recorded (not shown in graph), and a glucose pulse was added at 0 s. Timepoints were binned for every 5 s. Percentages are vol/vol. EtOH, ethanol. [a]FRET ratios were baseline-normalized.

per second to determine cAMP responses. The dynamics were comparable to the microscopy-obtained data (Figure 1D and Supplemental Figure S2). Of note, the complete population increases in cAMP levels, without showing any nonresponder, also not by the addition of low levels of glucose (i.e., 2 mM glucose, Supplemental Figure S2).

In summary, our developed yEPAC sensor can be used to reliably measure cAMP in single-yeast cells without adverse effects. Also, we show that our sensor can be used with flow cytometry, in addition to the conventional microscopy readouts, expanding its utility.

cAMP peak heights follow the Weber-Fechner law

After using saturating glucose amounts (Figure 1, B–D), we studied the response of cAMP levels to lower amounts of glucose. We pulsed ethanol-grown W303-1A cells with glucose ranging from 0 to 50 mM. Normalized peak heights of these transitions showed a saturating dose-response with a $K_{0.5}$ of 3.0 mM and a maximal peak height of 1.38 normalized FRET values (Figure 2A).

The dose-response data were generated against a background of zero glucose and indicated that yeast cells are able to detect low concentrations of glucose. However, we hypothesized that any advantage cells may reap from responding to a change in sugar availability will depend largely on the amount of sugar already in the environment (i.e., the background level). We therefore expected that the response to small glucose changes would depend on the background glucose level. Such behavior is described by the Weber-Fechner law (Ferrell, 2009), which states that the response of a sensory system depends not on the absolute but on the relative change of the signal. We therefore tested whether the magnitude of the glucose-induced cAMP peak heights scale with the relative change (i.e., fold change) of the glucose concentration instead of the absolute change. We incubated cells in media with various background concentrations of glucose and subsequently added different amounts of glucose (Figure 2, B, D–F). Indeed, we found comparable responses between transitions with the same relative but different absolute amounts of glucose pulsed (Figure 2B). Figure 2D

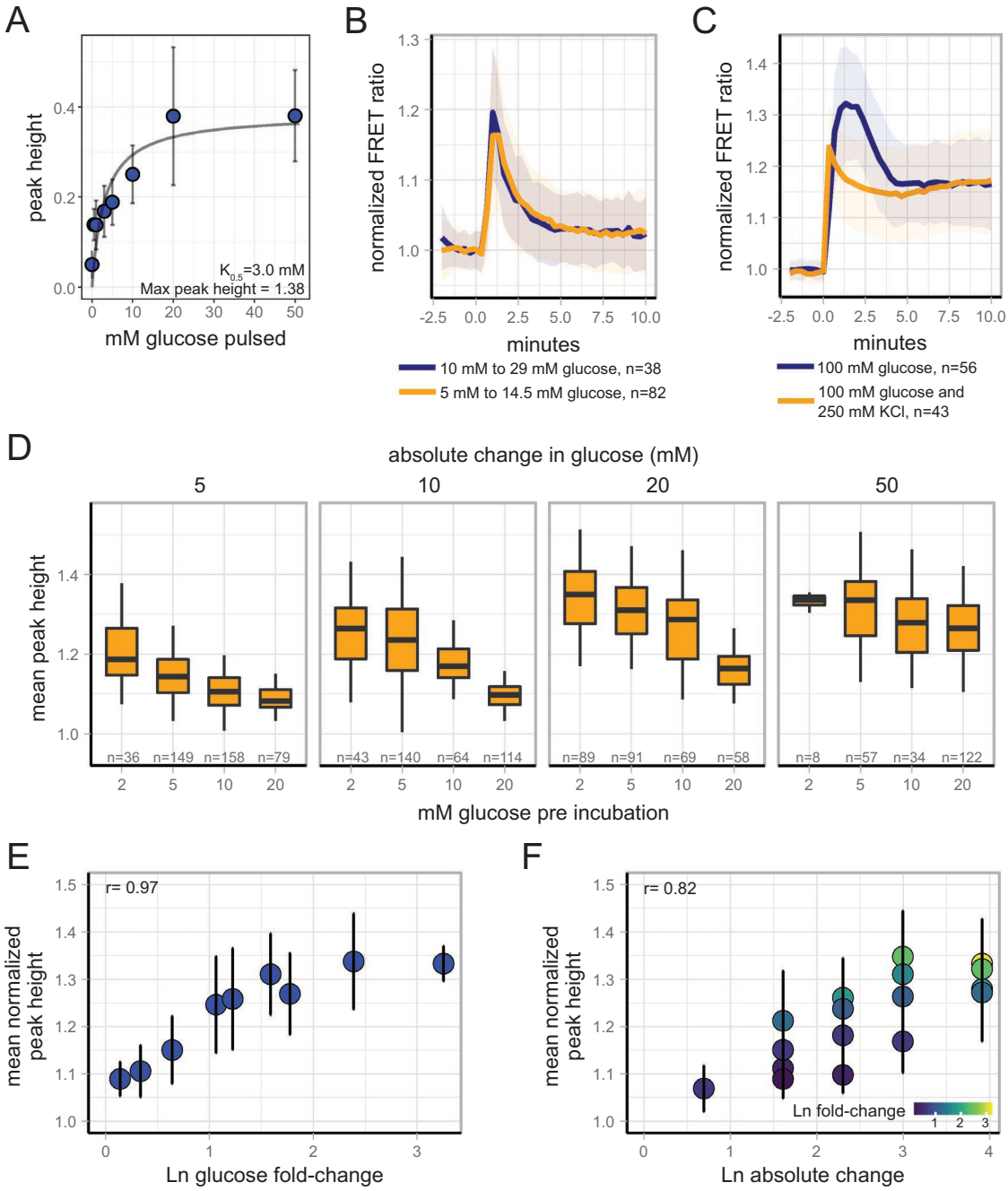

FIGURE 2: Dose-response and Weber-Fechner law experiments of cAMP. (A) W303-1A cells expressing yEPAC were grown on 1% ethanol and various glucose concentrations were pulsed. Fitting peak heights vs. the glucose concentration shows saturation kinetics with a $K_{0.5}$ of 3.0 mM. Dots indicate mean value, error bars indicate SD, and gray line shows the fit using Eq. 2. (B) W303-1A cells expressing yEPAC were preincubated at either 5 or 10 mM glucose and a 2.9-fold change of glucose was performed. Lines show mean response, shaded areas indicate SD. (C) W303-1A cells expressing yEPAC were grown on 1% EtOH and either 100 mM glucose or 100 mM glucose with 250 mM KCl was added. Lines show mean responses, and shaded areas indicate SD. (D) Population response of cAMP of cells expressing yEPAC. Cells were incubated at various initial amounts of glucose (depicted below each graph) and various amounts of glucose were added (depicted above each graph). Box plots indicate median values with quartiles, and whiskers indicate largest and smallest observation at 1.5 times the interquartile range. (E) Peak heights plotted against the natural logarithm of the fold change of various glucose transitions, dots indicate mean value, and error bars indicate SD. (F) Peak heights plotted against the absolute glucose change transitions, dots indicate mean value, error bars indicate SD, and color indicates the natural logarithm of the fold change.

depicts the normalized cAMP responses for various transitions. Differences in responses to 5 mM glucose were statistically significant between different background glucose levels, except between 10 and 20 mM preincubation at $\alpha = 0.05$ (TukeyHSD). At 10 mM absolute glucose change, this was also the case except between 2 and 5 mM preincubation; at 20 mM glucose change, all responses

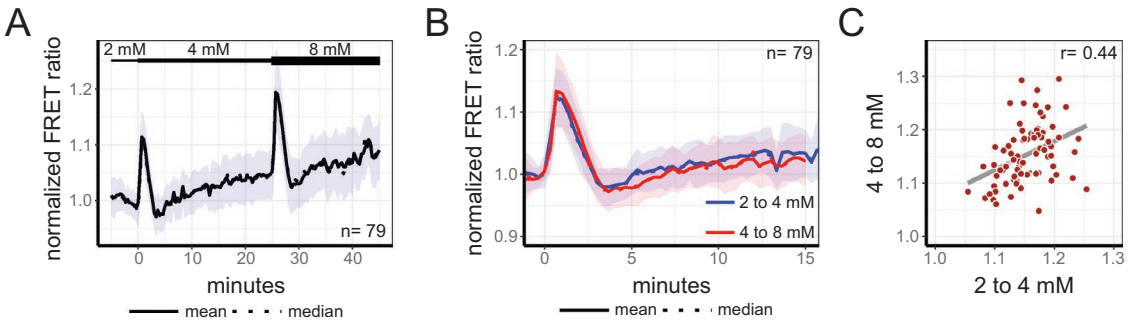

FIGURE 3: Weber-Fechner law of the same cells in time. (A) W303-1A cells expressing yEPAC were preincubated on 2 mM glucose. Afterward, cells were transitioned to 4 mM glucose at $t = 0$ min and transitioned again to 8 mM at $t =$ 25 min, resulting in a twofold change each time. Solid line shows the population mean response, and dotted line shows median response, normalized to the first 5 min. (B) Responses of the transitions performed in graph A, normalized to the last three frames before each transition. Solid line shows the population mean response, dotted line shows median response, and color indicates the transition. (C) Relation of normalized peak heights of single cells between the first and second transitions. Shaded areas indicate SD. Dots represent single cells, r-value shows the Spearman correlation coefficient ($p < 0.01$).

were statistically different, and with 50 mM glucose addition, only the glucose changes of 5 and 20 mM were statistically different at $\alpha = 0.05$ (TukeyHSD). These results indicate that normalized cAMP peak levels are dependent on the background glucose level.

Because systems that detect relative changes add up inputs with positive and negative responses (Adler and Alon, 2018), we also tested the application of two such inputs simultaneously. First, we identified salt stress as a negative input, as this reduced cAMP levels transiently (Supplemental Figure S3A). A combined addition of salt and glucose reduces the cAMP peak height that is observed with glucose addition alone (Figure 2C). This indeed indicates that the cAMP peak height can measure relative glucose changes (Adler and Alon, 2018). Furthermore, cells change cAMP peak heights based on their background level as discussed. The Weber-Fechner law has an effective range and does not hold at either very low or very high stimuli (Adler and Alon, 2018). We also found such a limit in the cAMP response during a transition from 100 to 400 mM glucose (Supplemental Figure S3B). Glucose sensing and transport approaches saturation at 100 mM of glucose. Therefore, it is conceivable that a further increase in glucose is not fully sensed and does not follow the Weber-Fechner law anymore. During this transition, the cAMP peak is hardly present and lower than the newly obtained baseline afterward (i.e., practically absent). Of note, timing of the peak heights did not differ between transitions (Supplemental Figure S3C). On a final note, the normalized peak heights relate better with the fold change in glucose than with the absolute glucose change (Figure 2, E and F).

Finally, we tested whether a fixed glucose fold change pulse applied successively to the same population would elicit a similar peak response (Figure 3). Indeed, we also found in this case the baseline-normalized peak height scales with the relative glucose change and not the absolute amount (Figure 3, A and B). For individual cells we found only a weak correlation between normalized peak heights of the first versus the second perturbation (Figure 3C). This indicates that at the single-cell level, the relative change is rather noisy, but at the population level, the response is robust. We further found that perturbations within a shorter timescale (i.e., every 10 min) showed deteriorated Weber-Fechner law responses (Supplemental Figure S4). In these short-term transitions, cells largely lose their ability to detect relative glucose changes. This suggests that the minimal timescales at which cells can adapt their glucose threshold is in the order of 20–30 min, and therefore the mechanism likely involves changes in protein expression.

In conclusion, we show that cAMP responses are sensitive to glucose changes when cells reside in low glucose environments. In high glucose environments, cAMP responses are rescaled, making the cAMP response relative to the current glucose levels cells are in.

cAMP responses are carbon-source transition dependent

The cAMP signaling cascade is well known and characterized for its transitions from nonfermentable carbon sources to glucose. However, less data are available for other transitions. Therefore, we quantified the cAMP response for transitions between a variety of carbon sources. W303-1A WT cells were grown in medium containing 1% ethanol (vol/vol), 1% glycerol (vol/vol), 100 mM pyruvate, or 111 mM galactose and subsequently pulsed with saturating amounts of glucose, fructose, galactose, mannose, or various oligosaccharides. This resulted in 18 different transitions for which the cAMP levels were monitored (Figure 4).

Among the added sugars, only sucrose, glucose, and fructose induced clear cAMP peaks. Addition of sucrose gave the highest peak and fructose the lowest. Cells pulsed with galactose or mannose did not show a cAMP peak. Mannose is known as an antagonist of Gpr1 (Kraakman *et al.*, 1999; Lemaire *et al.*, 2004) and galactose is not a Gpr1 activator, which suggests that Gpr1 regulates the height of the cAMP peak. Noteworthy is the observation that mannose-pulsed cells did show increased cAMP levels after 15 min, even though an initial peak response was absent. cAMP dynamics also depended on the pregrowth condition, with glycerol and pyruvate grown cells producing significantly higher cAMP peaks compared with EtOH- and galactose-grown cells (Wilcoxon test, $p < 0.01$). In line with the dynamic flow-FRET results, we did not observe subpopulations or nonresponders in most transitions (Supplemental Figure S5). Occasionally, we found for sugars other than glucose that some cells exhibited deviated cAMP dynamics compared with the population response. These cells show no cAMP peak or steadily increasing cAMP levels throughout the time-lapse recording. Therefore, cAMP signaling appears very robust for glucose transitions, but shows less robustness for other sugars.

Transitions from one primary carbon source to another can alter the maximal obtainable growth rate of cells. We wondered if cAMP peak heights could contain information about this new potential growth rate. Figure 4C indeed suggests such a relation: all data

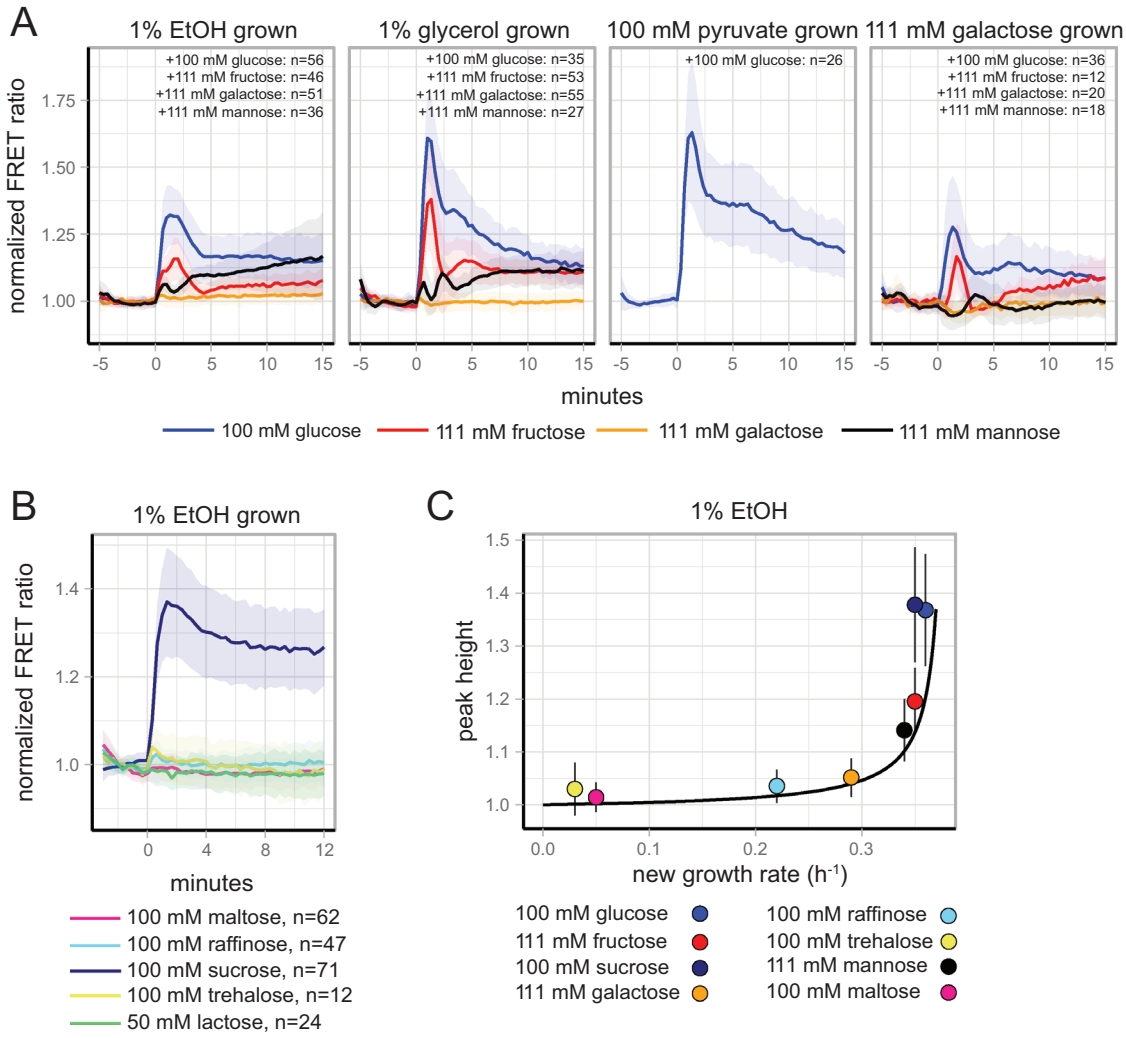

FIGURE 4: yEPAC FRET responses of various carbon transitions. (A) Cells growing on various nonfermentative carbon sources (depicted above each graph) were pulsed with various sugars, depicted by line color, at 0 min. Lines show mean FRET ratios, normalized to the baseline, and shaded areas indicate SD. (B) Cells growing on 1% ethanol were pulsed with various di- or trisaccharides and the FRET responses were recorded. Lines show mean FRET ratios, normalized to the baseline, shaded areas indicate SD, and sugar was added at $t = 0$ min. (C) Peak heights of the transitions shown in A and B plotted against the maximal growth rate that can be obtained with the added carbon sources. Points show population mean, error bars indicate SD, and solid line shows a glucose-dependent curve (obtained by plotting the dose-response kinetics against Monod kinetics).

appear to lie on a curve. This curve fits very well with a glucose-dependent curve obtained when the dose-response kinetics of Figure 2A (max peak height 1.38 and $K_{0.5} = 3.0$ mM) is plotted against the growth rate inferred from published Monod kinetics with a maximal growth rate of 0.37 h^{-1} and a K_s of 0.1 mM (Canelas *et al.*, 2011). Note that the cAMP peak height shows a sharp increase when a growth rate higher than 0.3 h^{-1} can be obtained, which is around the onset of overflow metabolism (Van Hoek *et al.*, 1998).

In summary, our results show that the cAMP dynamics are context dependent, and that—at least for transitions from EtOH to sugars tested here—the peak height corresponds to the growth rate that can be achieved in the new environment.

cAMP dynamics are dependent on Gpr1 signaling and sugar metabolism and differ between strains

Last, we examined which components of the signaling cascade affect the cAMP peak during transitions. In addition, we tested cAMP responses among three widely used strains (W303-1A, Cen.PK, and BY4743) to see whether their genetic backgrounds affect cAMP signaling. cAMP signaling mutants were grown on medium containing 1% EtOH and pulsed with 2% glucose (Figure 5). Deletion of Gpr1, all three glucose phosphorylating enzymes (hxk1Δ, hxk2Δ, glk1Δ triple mutant), or the mutation in Cyr1 ($Cyr1^{K1876M}$) affected the transient peak in cAMP. Noteworthy, the hxk1Δ, hxk2Δ, glk1Δ mutant still showed a clear cAMP peak (although decreased compared with WT). This mutant does not display transient intracellular acidification on glucose addition (since glucose cannot be metabolized), indicating that cAMP peak generation does not solely rely on acidification, or metabolism, for that matter. Deletion of another input via the membrane-bound Gpr1 sensor had a similar effect on the cAMP peak response. Since these two branches are known to regulate cAMP responses, we hypothesize that the residual cAMP response for both mutants are caused by the other cAMP signaling branch that is still functioning. Last, the cAMP response of the three strains

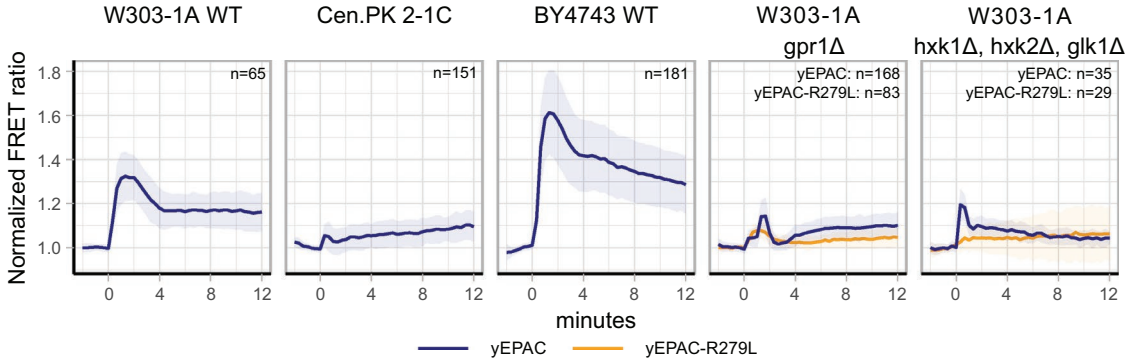

FIGURE 5: yEPAC FRET responses of various (signaling) mutants. The various strains were pulsed with 100 mM glucose at 0 min. Lines show mean FRET ratios, normalized to the baseline, colors indicate sensor type, and shaded areas indicate SD.

tested also showed different responses, with BY4743 giving the highest cAMP response, followed by W303-1A. Cen.PK 2-1C did not show a clear transient peak, but shows a gradual increase of cAMP levels in time.

DISCUSSION

We present a FRET-based biosensor for dynamic, single-cell cAMP detection in yeast. Although a different FRET-based cAMP EPAC biosensor for budding yeast was published previously (Bermejo *et al.*, 2013; Colombo *et al.*, 2017), we believe that our yEPAC has significant improvements. It shows a high FRET range, up to a normalized ratio change of 1.7 (Figure 1B). Furthermore, the growth assays show that the sensor has no adverse effects on yeast physiology (Supplemental Figure S1F, growth rates of 0.39 h^{-1} and 0.37 h^{-1} on glucose, 0.27 h^{-1} and 0.27 h^{-1} on galactose, and 0.19 h^{-1} and 0.18 h^{-1} on ethanol for the empty plasmid and the yEPAC sensor, respectively). The slight difference in cAMP affinity of yEPAC compared with the original sensor could be caused by the different acceptor used, which possibly changes conformation of the sensor slightly, or could be caused by differences in characterization conditions such as the host species and the used buffers. Signaling mutants and the nonresponsive yEPAC variant showed good cAMP selectivity of the sensor. However, we found a slight bias of basal FRET levels of yEPAC-R279L at various growth rates (Supplemental Figure S1G). The minor effect of growth rate on basal FRET levels (a 15% decrease in baseline FRET of ethanol-grown cells compared with glucose-grown cells) does not largely affect the FRET responses. The origin of this bias is currently unknown and subject for future research and sensor improvements. The obtained flow cytometry data gave a high temporal resolution compared with the conventional used cAMP assays. These results showed a clear secondary peak (Supplemental Figure S2) at high glucose concentrations. This peak was also present (e.g., Figure 4A), but not consistently observed, in the microscopy dataset. This oscillatory behavior is in line with predictions from modeling efforts, but was not further explored in this study (Besozzi *et al.*, 2012).

Of note, neither flow cytometry nor microscopy showed clear nonresponders for glucose transitions (Figure 1 and Supplemental Figure S5). However, we observed some heterogeneity in transitions with sugars that do not activate Gpr1 (Lemaire *et al.*, 2004). Therefore, we hypothesize that this heterogeneity occurs from variation in the metabolism of the sugar, as observed before with carbon-source transitions (van Heerden *et al.*, 2014; Botman *et al.*, 2020). These results show that the cAMP signaling cascade is robust, in contrast to what was found for pH (van Heerden *et al.*, 2014) and recently for intracellular ATP dynamics as well (Botman *et al.*, 2020). Apparently, as shown earlier (Youk and van Oudenaarden, 2009), signaling glucose or metabolizing it are different challenges to yeast cells.

In nature, yeast cells likely encounter large fluctuations in glucose availability, ranging from complete absence to saturating amounts of glucose. Until now, it was unknown how cAMP signaling reacts to a glucose increase when glucose is already present in the environment. We tested these transitions and found that cAMP peak heights seem to measure glucose changes relative to the background level of glucose, a property known as the Weber-Fechner law. Our analyses to test for Weber-Fechner law assume that each cell performs baseline-normalization. This could give an extra benefit by reducing variability among cells (Lee *et al.*, 2014; Frick *et al.*, 2017; Kamino *et al.*, 2017; Adler and Alon, 2018). However, cells need time to establish a baseline between successive glucose additions, since shortening the period between glucose additions no longer gave scaling of the cAMP peak height with the relative fold change (Supplemental Figure S4).

To reliably test for Weber-Fechner law, cAMP levels should be below saturation values of the yEPAC sensor. We validated this by comparing the normalized peak heights in response to saturating glucose amount (i.e., 50 mM glucose) when cells are preincubated at 2, 5, 10, and 20 mM glucose (Figure 2D). Normalized peak heights were comparable, indicating that cAMP levels did not yet saturate the sensor. Furthermore, preincubation with 2 to 20 mM glucose did not specifically affect the yEPAC sensor, as the yEPAC-R279L hardly shows any response after pulsing with 100 mM glucose (Supplemental Figure S6), which is at least five times more than used for Weber-Fechner law characterization. Our data therefore indicate that the cAMP pathway in yeast cells can detect (and adapt to) small glucose additions when glucose levels are low, but does not signal this change when glucose levels are already high. When cells are already fully fermentative, growing on glucose, the peak cannot indicate an increase in growth rate, but rather may signal how much sugar is present and whether or not cells should keep investing in fermentation and ribosomal biosynthesis.

This is different when we added different carbon sources to fully respiratory, ethanol pregrown cells. At this background, a consistent relation between peak height and the prospective growth rate on the pulsed sugar was found, for different sugars, and fitted the predicted growth rate for different glucose concentrations, based on Monod growth kinetics. This suggests that the peak height informs about growth. The cAMP signaling cascade is generally considered to mediate a switch to a fermentative (i.e., high growth rate) mode. This was consistent with our data, where cAMP peak height

Strain	Genotype	Source
W303-1A WT	MATa, leu2-3/112, ura3-1, trp1-1, his3-11/15, ade2-1, can1-100	J. Thevelein, Katholieke Universiteit Leuven, Belgium
YSH757	W303-1A glk1Δ::LEU2 hxk1Δ::HIS hxk2Δ::LEU2	Stefan Hohmann, Chalmers University of Technology, Gotenburg, Sweden
W303-1A gpr1Δ	W303-1A gpr1Δ::LEU2	Joris Winderickx, Katholieke Universiteit Leuven, Belgium.
W303-1A Cyr1^{K1876M}	W303-1A Cyr1^{K1876M}	Joris Winderickx, Katholieke Universiteit Leuven, Belgium.
Cen.PK 2-1C	MATa, his3D1, leu2-3_112, ura3-52, trp1-289, MAL2-8c, SUC2	In house
BY4743 WT	MATa/α, his3Δ1/his3Δ1, leu2Δ0/leu2Δ0 LYS2/lys2Δ0, met15Δ0/MET15 ura3Δ0/ura3Δ0	In house

TABLE 1: *S. cerevisiae* strains used in this paper.

increased sharply around the onset of fermentation, that is, under conditions that generate a growth rate higher than 0.3 h^{-1} (Figure 4C). However, our results also show that cells without a clear cAMP peak (e.g., mannose pulsed cells) still obtain a high growth rate, without displaying a transient cAMP peak. Also, the industrially important CEN.PK strain that has the K1876M mutation in Cyr1 (Vanhalewyn *et al.*, 1999) does not show a peak but does ferment. Therefore, although we find clear and interesting relationships, their functional implications remain to be fully elucidated.

The cAMP responses to various other sugar transitions and in signaling mutants show that cAMP dynamics are complex and highly context dependent. We could infer several features about cAMP signaling from these data.

First, nine sugars were tested and only sucrose (giving the highest peak) and its breakdown products, glucose and fructose, induced a cAMP peak. It is remarkable that yeast developed a signaling cascade for only these sugars. On the other hand, sucrose is often the end product of plant photosynthesis and therefore one of the most abundant sugars in plants (Ruan, 2014). In nature, yeast resides on plants or fruit, and sensing extracellular sucrose to consume conceivably improves yeast's fitness.

Second, the data indicate that a cAMP peak is generated when either the initial metabolism of a sugar is sufficiently rapid or the Gpr1 is activated. Combined activation is needed to achieve a maximal peak response. We found that fructose, which does not interact with Gpr1 (Lemaire *et al.*, 2004), does induce a cAMP peak. In the case of fructose, the peak is lower than peaks induced by the Gpr1 agonists sucrose or glucose, pointing to the amplifying effect of combined activation.

In stark contrast to the peak responses triggered by sucrose, glucose, and fructose, mannose, which is an antagonist of Gpr1, does not show any cAMP peak. One explanation for the absence of a peak is signal-dampening through Gpr1 inhibition. Another explanation is that mannose gets transported much more slowly, since the hexose transporters have a lower V_{max} and a higher K_m for mannose compared with glucose and fructose, which likely reduce the initial uptake rate of mannose (Reifenberger *et al.*, 1997; Reijenga *et al.*, 2001). Still, we found that mannose does trigger a gradual increase in cAMP levels shortly after its addition, which could indicate Ras activation through an increased glycolytic flux (Peeters *et al.*, 2017). Accordingly, the addition of galactose, which does not interact with Gpr1 and is not considered a rapidly fermentable carbon source, does not induce a cAMP peak and does not yet show signs of a gradual increase in cAMP levels shortly after its addition. Indeed, cells growing on ethanol or glycerol are not immediately ready to metabolize galactose (Lohr *et al.*, 1995), and we expect the cAMP levels to gradually rise with the induction of galactose metabolism. A differential response to mannose by galactose- or ethanol-grown cells further underscores the effect of pregrowth conditions on the ability of cells to sense and respond to sudden sugar transitions. Mannose did not show the gradual increase in cAMP levels in galactose-grown cells as it did in ethanol-grown cells. Galactose growth suppresses the expression of various high-affinity hexose transporters, such as HXT6 and 7, compared with growth on ethanol or glycerol (Ozcan and Johnston, 1995; Paulo *et al.*, 2015, 2016). The mannose uptake rate is therefore expected to be much lower in galactose-grown cells than ethanol- or glycerol-grown cells, which may explain these observations. The response of the glucose and fructose addition to galactose-grown cells is expected as galactose-grown cells have a higher capacity to metabolize these sugars, which induces a cAMP peak (Herrero *et al.*, 1995; Reifenberger *et al.*, 1997; Rolland *et al.*, 2001; Maier *et al.*, 2002; Botman *et al.*, 2020). We confirm that the cAMP peaks clearly originate partly from both the metabolism of the sugar and the Gpr1 receptor, as described before (Eraso *et al.*, 1987; Yun *et al.*, 1998; Kraakman *et al.*, 1999). In line with previous studies, our data indicate that intracellular acidification is not a requisite as the hxk1Δ, hxk2Δ, glk1Δ shows no intracellular acidification (due to the absence of sugar phosphorylation) and still shows cAMP production (Eraso *et al.*, 1987; Thevelein *et al.*, 1987; Colombo *et al.*, 1998). Finally, using the yEPAC sensor, we could conveniently compare cAMP responses between strains. As expected, the Cen.PK strain, which has the Cyr1^{K1876M} mutation (Vanhalewyn *et al.*, 1999), lacks the cAMP peak. In addition, the BY4743 strain showed a higher response on glucose addition compared with W303-1A and slower recovery. The reason for this is unknown and may be the result of differences in glycolytic flux (by the hexokinases), sensing (by Gpr1), cAMP breakdown, or other unknown differences in their genetic background.

Overall, yEPAC enabled us for the first time to investigate single-cell cAMP dynamics and elucidate conveniently various input-output relations during various carbon-source transitions. This gave important new insights: the normalized peak height seems to be a signal for future growth rate on the pulsed sugar and is only produced when cells should switch to fermentative growth. Possibly, the peak height functions as a switch for rewiring to fermentable metabolism.

MATERIAL AND METHODS

Request a protocol through *Bio-protocol*.

Fluorescent protein plasmids construction

The FRET pairs mCherry-T2A-mTurquoise2 (mTq2), tagRFP-T2A-mTq2, tagRFPT-T2A-mTq2, and tdTomato-T2A-mTq2 in pDRF1-GW were previously constructed (Botman *et al.*, 2019). mCherry-mTq2, tagRFP-mTq2, and tagRFPT-mTq2 in a Clontech-style C1 mammalian expression vector were obtained from Mastop *et al.* (2017), digested using *Nhe*I and *Not*I (New England Biolabs, Ipswich, MA), and ligated with T4 ligase (New England Biolabs) in the yeast expression vector pDRF1-GW (Botman *et al.*, 2019), digested with the same restriction enzymes.

mTq2 in pDRF1-GW was created by performing a PCR, using KOD polymerase (Merck-Millipore, Burlington, MA) on mTq2-C1 using forward primer 5′-AGGTCTATATAAGCAGAGC-3′ and reverse primer 5′-TAGCGGCCGCTTACTTGTACAGCTCGTCCATG-3′. Next, the product and pDRF1-GW were digested with *Nhe*I and *Not*I and the PCR product was ligated into pDRF1-GW using T4 ligase, generating mTq2 in pDRF1-GW.

yEPAC construction

mTq2Δ-Epac (CD,ΔDEP)-cp173Venus-cp173Venus (Epac-SH188) was a kind gift of Kees Jalink. A PCR with KOD polymerase was performed on tdTomato-C1, using forward primer 5′-TAGAGCTCATGGTGAGCAAGGGCGAGG-3′ and reverse primer 5′-GCGGCCGCTTACTTGTACAGCTCGTCCATGCCG-3′. Next, both the PCR product and Epac-SH188 were digested using *Sac*I and *Not*I (New England Biolabs). The PCR product was ligated into Epac-SH188 using T4 ligase, replacing cp173Venus-cp173Venus for tdTomato. The adapted sensor and pDRF1-GW were digested using *Nhe*I and *Not*I and the sensor was ligated into pDRF1-GW, generating yEPAC (mTurquoise2Δ-Epac(CD,ΔDEP)-tdTomato in pDRF1-GW).

Yeast transformation

Strains used in this study are described in Table 1. These strains were transformed exactly as described by Gietz and Schiestl (2007).

In vitro characterization

W303-1A WT cells transformed with pDRF1-GW, and yEPAC were grown overnight at 200 rpm and 30°C in 1× yeast nitrogen base (YNB) medium without amino acids (Sigma-Aldrich, St. Louis, MO) containing 100 mM glucose (Boom BV, Meppel, The Netherlands), 20 mg/l adenine hemisulfate (Sigma-Aldrich), 20 mg/l L-tryptophan (Sigma-Aldrich), 20 mg/l L-histidine (Sigma-Aldrich), and 60 mg/l L-leucine (SERVA Electrophoresis GmbH, Heidelberg, Germany). The next day, cells were diluted and grown to an OD_{600} of approximately 3 in 50 ml of the same medium. Next, cells were kept on ice and washed twice in ice-cold 20 ml 0.01 M KH_2PO_4/K_2HPO_4 buffer at pH 7 containing 0.75 g/l EDTA (AppliChem GmbH, Darmstadt, Germany). After the last wash step, cells were resuspended in 2 ml of 0.01 M KH_2PO_4/K_2HPO_4 buffer containing 0.75 g/l EDTA. Cells were washed twice in 1 ml of ice-cold 0.1 M KH_2PO_4/K_2HPO_4 buffer at pH 7.4 containing 0.4 g/l $MgCl_2$ (Sigma-Aldrich). Cells were transferred to screw cap tubes prefilled with 0.75 g of glass beads (425–600 µm) and lysed using a FastPrep-24 5G (MP Biomedicals, Santa Ana, CA) with 8 bursts at 6 m/s and 10 s per burst. Afterward, the lysates were centrifuged for 15 min at 21,000 × *g* and the cell-free extracts were snap-frozen in liquid nitrogen and stored at –80°C for later use.

Per sample, 5 wells of a black 96-well microtiter plate (Greiner Bio-One) were filled with 40 µl of cell-free extract. Fluorescence spectra were recorded after successive additions of cAMP (Sigma-Aldrich) using a CLARIOstar platereader (BMG Labtech, Ortenberg, Germany). Spectra were recorded with 430/20 nm excitation and 460–660 nm emission (10 nm bandwidth). Fluorescence spectra were corrected for background fluorescence (by correcting for fluorescence of W303-1A WT expressing the empty pDRF1-GW plasmid), and FRET ratios were calculated by dividing donor over acceptor fluorescence. The data were fitted to the Hill equation (Eq. 1; Ponsioen *et al.*, 2004), with cAMP denoting the cAMP concentration, K_d the dissociation constant, and *n* the Hill-coefficient.

$$FRET\ ratio = \frac{cAMP^n}{K_d^n + cAMP^n} \quad (1)$$

Concanavalin A solution

Concanavalin A (ConA) was prepared as described by Hansen *et al.* (2015). In brief, 5 mg of ConA (Type IV, Sigma-Aldrich) was dissolved in 5 ml PBS at pH 6.5, 40 ml H_2O, 2.5 ml of 1 M $MnCl_2$, and 2.5 ml of 1 M $CaCl_2$ and stored at –80°C.

Microscopy

Strains used in this study are described in Table 1. These strains (expressing yEPAC in pDRF1-GW, or EPAC2-camps in pYX212) were grown overnight at 200 rpm and 30°C in 1× YNB medium, without amino acids, containing 20 mg/l adenine hemisulfate, 20 mg/l L-tryptophan, 20 mg/l L-histidine, 60 mg/l L-leucine and either 1% ethanol (vol/vol, VWR International, Radnor, PA), 1% glycerol (vol/vol, Sigma-Aldrich), 100 mM pyruvate (Sigma-Aldrich), or 111 mM galactose (Sigma-Aldrich). Next, cells were diluted in the same medium and grown to an OD600 of maximally 1.5 and with minimal five cell divisions. The cultures were transferred to a 6-well microtiter plate containing coverslips pretreated ConA to immobilize the cells. Afterward, the coverslip was put in an Attofluor cell chamber (ThermoFisher Scientific, Waltham, MA) and 1 ml of fresh medium was added. Samples were imaged with a Nikon Ti-eclipse widefield fluorescence microscope (Nikon, Minato, Tokio, Japan) at 30°C equipped with a TuCam system (Andor, Belfast, Northern Ireland) containing 2 Andor Zyla 5.5 sCMOS Cameras (Andor) and a SOLA 6-LCR-SB power source (Lumencor, Beaverton, OR). Fluorescent signals were obtained using a 438/24 nm excitation filter. The emission was separated by a 552 nm long-pass (LP) dichroic filter in a TuCam system. A 483/32 nm and 593/40 nm emission filter-pair was used for the detection of donor and acceptor emission, respectively (all filters from Semrock, Lake Forest, IL). Perturbations were performed by adding 1× YNB medium containing the same amino acids as described before with 10× concentrated carbon source or KCl to the cell chamber to the desired concentration. Per condition, at least two biological replicates were obtained. Cells were segmented and fluorescence was measured with an in-house Fiji macro (National Institutes of Health, Bethesda, MD).

Growth experiments

Cells expressing pDRF1-GW and yEPAC were grown to midlog as described for microscopy with medium containing 1% ethanol. Next, cells were washed and resuspended to an OD_{600} of 1 with the same medium with the carbon source omitted. Cells were transferred to an OD of 0.05 in a 48-well microtiter plate containing 480 µl of fresh medium with 0.1% ethanol, 10 mM galactose, or 10 mM glucose. The cells were grown in a CLARIOstar plate reader at 30°C and 700 rpm orbital shaking. OD_{600} was measured every 5 min. Growth rates were calculated using a sliding window and are determined according to Eq. 2 with µ denoted as the growth rate and *t* as timepoints in hours,

$$\mu = \frac{Log\left(OD_{600_{t_2}}\right) - Log\left(OD_{600_{t_1}}\right)}{t_2 - t_1} \quad (2)$$

Fluorescence lifetime imaging and spectral imaging

W303-1A WT cells expressing mCherry-mTq2, mCherry-T2A-mTq2, tagRFP-mTq2, tagRFP-T2A-mTq2, tagRFPT-mTq2, tagRFPT-T2A-mTq2, tdTomato-mTq2, and tdTomato-T2A-mTq2 were grown for at least 2 wk on 2% agarose plates containing 6.8 g/l YNB without amino acids, 100 mM glucose, 20 mg/l adenine hemisulfate, 20 mg/l L-tryptophan, 20 mg/l L-histidine, and 60 mg/l L-leucine. Frequency domain FLIM was performed as described before (Mastop *et al.*, 2017). Briefly, 18 phase images were obtained with a RF-modulated image intensifier (Lambert Instruments II18MD, Groningen, The Netherlands) set at a frequency of 75.1 MHz coupled to a CCD camera (Photometrics HQ, Tucson, AZ) as detector. mTq2 was excited using a directly modulated 442-nm laser diode (PicoQuant, Berlin, Germany). Emission was detected using a 480/40-nm filter. The lifetimes were calculated based on the phase shift of the emitted light ($\tau\phi$). Per sample, three replicates were recorded.

Emission spectra of a donor-acceptor fusion protein or unfused equimolar expressed donor and acceptor were acquired as described previously (Mastop *et al.*, 2017). In brief, excitation was at 436/20 nm and the emission was passed through a 80/20 (transmission/reflection) dichroic mirror and a 460-nm LP filter. Individual spectra were corrected for expression level by quantifying the intensity of the acceptor by excitation at 546/10 nm and detection with a 590-nm LP filter. Per sample, three replicates were measured.

Flow cytometry

W303-1A strains expressing yEPAC, pDRF1-GW, and mTq2 were grown as described for microscopy. Flow cytometry was performed using an BD INFLUX cell sorter (Becton Dickinson, Franklin Lakes, NJ), with a 140-µm nozzle and a sheath pressure of 6 psi to run the samples. The sorter was equipped with a 200 mW Solid State 488-nm laser focused on pinhole 1, a 75 mW Solid State 561-nm laser focused on pinhole 3 with a laser delay of 18.17 µs, and a 100 mW Solid State 445-nm laser focused on pinhole 5 with a laser delay of 37.11 µs. PMTs (photo multiplier tubes) for the 445-nm laser and the 488-nm laser were assimilated in trigon detector arrays that use serial light reflections—moving from the longest wavelengths to the shortest—to collect the dimmest emission signals first. The 445-nm trigon array was configured with a 610/20-nm bandpass filter in detector A and a 520/35-nm bandpass filter (preceded by a 502-nm LP filter) in detector B. The 488 trigon array was configured with a 610/20-nm bandpass (preceded by a 600LP) in detector A, a 530/40-nm bandpass (preceded by a 520 LP) in detector B, and a 488/10-bandpass in detector C (SSC). PMTs for the 561 laser were assimilated in an octagon detector array. Acceptor emission was measured in detector D which was filtered with a 610/20 bandpass (preceded by a 600LP). Per condition, at least two biological replicates were obtained. All events were corrected for background fluorescence (median fluorescence of cells expressing pDRF1-GW), bleedtrough corrected (median fluorescence of cells expressing mTq2 only in the acceptor channel) and filtered for saturating or low fluorescence and scatter values. The effect of sensor expression on FRET ratios was calculated by plotting FRET ratios against tdTomato expression, obtained with the 561-nm laser and a 610/20-nm bandpass filter.

pH sensitivity

Cells expressing yEPAC-R279L and mVenus-mTq2 were grown to an OD_{600} of maximally 1.5 in YNB medium containing 100 mM glucose. Cells were washed 3× and resuspended in Citric Acid/Na_2HPO_4 buffer at various pH containing 2 mM of the ionophore 2,4-dinitrophenol to equilibrate pH levels. Afterward, FRET ratios were recorded using a widefield microscope as described before.

Data availability and analysis

All data are available online: http://dx.doi.org/10.17632/mknc4bn793.1. Data were analyzed and visualized using R version 3.5.1 (R Foundation for Statistical Computing, Vienna, Austria). For analysis, moving and dead cells were manually removed. Additionally, cells with low fluorescence (i.e., below 50 A.U. fluorescence counts) were excluded. Next, acceptor fluorescence was corrected for bleedthrough (12% of total donor fluorescence) and FRET ratios were normalized to the mean FRET ratio before the perturbation (baseline). Dose-response kinetics were fitted using Eq. 3 with $Peak_{max}$ denoted as the maximal peak height that can be obtained, glucose as the amount of glucose pulsed, and $K_{0.5}$ as the glucose amount that induces half the maximal peak height.

$$Peak\ height = \frac{Peak_{max} \cdot glucose}{K_{0.5} + glucose} \quad (3)$$

MATERIAL REQUESTS

Requests for the yEPAC sensor should be addressed to Kees Jalink (Division of Cell Biology, Netherlands Cancer Institute, Plesmanlaan 121, 1066CX Amsterdam, The Netherlands, email k.jalink@nki.nl). Other material requests should be addressed to Bas Teusink (email: b.teusink@vu.nl).

ACKNOWLEDGMENTS

We thank Kees Jalink (Division of Cell Biology, The Netherlands Cancer Institute) for sharing mTurquoise2Δ-Epac(CD,ΔDEP)-cp173Venus-cp173Venus (Epac-SH188). We thank Juan Garcia Vallejo and Cora Chadick (Molecular Cell Biology & Immunology, VUmc) for his help with flow cytometry. We are also grateful to Sonia Colombo and V.O. Nikolaev for sharing YFP-EPAC2-CFP with us. We thank Joris Winderickx (Functional Biology, KU Leuven) and Marco Siderius (Amsterdam Institute for Molecules, Medicines and Systems [AIMMS], Division of Medicinal Chemistry) for sharing W303-1A mutant strains. We thank Daan de Groot and Philipp Savakis for fruitful discussions. This work was supported by the NWO VICI grant 865.14.005

REFERENCES

Adler M, Alon U (2018). Fold-change detection in biological systems. Curr Opin Syst Biol 8, 81–89.

van Aelst L, Boy-marcotte E, Camonis JH, Thevelein JM, Jacquet M (1990). The C-terminal part of the CDC25 gene product plays a key role in signal transduction in the glucose-induced modulation of CAMP level in Saccharomyces cerevisiae. Eur J Biochem 6680, 675–680.

van Aelst L, Jans WH, Thevelein M (1991). Involvement of the CDC25 gene product in the signal transmission pathway of the glucose-induced RAS-mediated cAMP signal in the yeast Saccharomyces cerevisiae. J Gen Microbiol 137, 341–349.

Altschuler SJ, Wu LF (2010). Cellular heterogeneity: do differences make a difference? Cell 141, 559–563.

Bermejo C, Haerizadeh F, Sadoine MSC, Chermak D, Frommer WB (2013). Differential regulation of glucose transport activity in yeast by specific cAMP signatures. Biochem J 452, 489–497.

Besozzi D, Cazzaniga P, Pescini D, Mauri G, Colombo S, Martegani E (2012). The role of feedback control mechanisms on the establishment of oscillatory regimes in the Ras/cAMP/PKA pathway in S. cerevisiae. EURASIP J Bioinforma Syst Biol 2012, 10.

Beullens M, Mbonyi K, Geerts L, Gladines D, Detremerie K, Jans AW, Thevelein JM (1988). Studies on the mechanism of the glucose-induced cAMP signal in glycolysis and glucose repression mutants of the yeast Saccharomyces cerevisiae. Eur J Biochem 172, 227–231.

Botman D, de Groot DH, Schmidt P, Goedhart J, Teusink B (2019). In vivo characterisation of fluorescent proteins in budding yeast. Sci Rep 9, 2234.
Botman D, van Heerden JH, Teusink B (2020). An improved ATP FRET sensor for yeast shows heterogeneity during nutrient transitions. ACS Sensors, acssensors.9b02475.
Broek D, Toda T, Michaeli T, Levin L, Birchmeier C, Zoller M, Powers S, Wigler M (1987). The S. cerevisiae CDC25 gene product regulates the RAS/Adenylate Cyclase Pathway. Cell 48, 789–799.
Canelas AB, Ras C, ten Pierick A, van Gulik WM, Heijnen JJ (2011). An in vivo data-driven framework for classification and quantification of enzyme kinetics and determination of apparent thermodynamic data. Metab Eng 13, 294–306.
Casperson GF, Walker N, Bourne HR (1985). Isolation of the gene encoding adenylate cyclase in *Saccharomyces cerevisiae*. Proc Natl Acad Sci USA 82, 5060–5063.
Colombo S, *et al*. (1998). Involvement of distinct G-proteins, Gpa2 and Ras, in glucose- and intracellular acidification-induced cAMP signalling in the yeast Saccharomyces cerevisiae. EMBO J 17, 3326–3341.
Colombo S, Broggi S, Collini M, D'Alfonso L, Chirico G, Martegani E (2017). Detection of cAMP and of PKA activity in *Saccharomyces cerevisiae* single cells using Fluorescence Resonance Energy Transfer (FRET) probes. Biochem Biophys Res Commun 487, 594–599.
Delvigne F, Zune Q, Lara AR, Al-Soud W, Sørensen SJ (2014). Metabolic variability in bioprocessing: Implications of microbial phenotypic heterogeneity. Trends Biotechnol 32, 608–616.
Dihazi H, Kessler R, Eschrich K (2003). Glucose-induced stimulation of the Ras-cAMP pathway in yeast leads to multiple phosphorylations and activation of 6-phosphofructo-2-kinase. 6275–6282.
Dong J, Bai X (2011). The membrane localization of Ras2p and the association between Cdc25p and Ras2-GTP are regulated by protein kinase A (PKA) in the yeast Saccharomyces cerevisiae. FEBS Lett 585, 1127–1134.
Engelberg D, Simchen G, Levitzki A (1990). In vitro reconstitution of cdc25 regulated S. cerevisiae adenylyl cyclase and its kinetic properties. EMBO J 9, 641–651.
Eraso P, Gancedo JM (1985). Use of glucose analogues to study the mechanism of glucose-mediated cAMP increase in yeast. FEBS Lett 191, 51–54.
Eraso P, Mazón MJ, Gancedo JM (1987). Internal acidification and cAMP increase are not correlated in Saccharomyces cerevisiae. Eur J Biochem 165, 671–674.
Ferrell JE (2009). Signaling motifs and Weber's Law. Mol Cell 36, 724–727.
Frick CL, Yarka C, Nunns H, Goentoro L (2017). Sensing relative signal in the Tgf-β/Smad pathway. Proc Natl Acad Sci 114, E2975–E2982.
Gietz RD, Schiestl RH (2007). Quick and easy yeast transformation using the LiAc/SS carrier DNA/PEG method. Nat Protoc 2, 35–37.
Hansen AS, Hao N, O'Shea EK (2015). High-throughput microfluidics to control and measure signaling dynamics in single yeast cells. Nat Protoc 10, 1181–1197.
Hardy TA, Huang D, Roach PJ (1994). Interactions between cAMP-dependent and SNF1 protein kinases in the control of glycogen accumulation in *Saccharomyces cerevisiae*. J Biol Chem 269, 27907–27913.
Herrero P, Galíndez J, Ruiz N, Martínez-Campa C, Moreno F (1995). Transcriptional regulation of the *Saccharomyces cerevisiae* HXK1, HXK2 and GLK1 genes. Yeast 11, 137–144.
Hixsons CS, Krebs EG (1980). Characterization of a cyclic AMP-binding protein from baker's yeast. J Biol Chem 255, 2137–2145.
Van Hoek P, Van Dijken JP, Pronk JT (1998). Effect of specific growth rate on fermentative capacity of baker's yeast. Appl Environ Microbiol 64, 4226–4233.
Hofmann E, Bedri A, Kessler R, Kretschmer M, Schellenberger W (1989). 6-Phosphofructo-2-kinase and fructose-2,6-bisphosphatase from *Saccharomyces cerevisiae*. Adv Enzyme Regul 28, 283–306.
Johnson KE, Cameron S, Wiglers M, Zollers MJ (1987). Expression in *Escherichia coli* of B C Y l, the regulatory subunit of cyclic AMP-dependent protein kinase from *Saccharomyces cerevisiae*. J Biol Chem 262, 8636–8642.
Kamino K, Kondo Y, Nakajima A, Honda-Kitahara M, Kaneko K, Sawai S (2017). Fold-change detection and scale invariance of cell–cell signaling in social amoeba. Proc Natl Acad Sci 114, E4149–E4157.
Kataoka T, Broek D, Wigler M (1985). DNA sequence and characterization of the *S. cerevisiae* gene encoding adenylate cyclase. Cell 43, 493–505.
Kim J, Roy A, Ii DJ (2013). Biochimica et Biophysica Acta The glucose signaling network in yeast. Biochim Biophys Acta Gen Subj 1830, 5204–5210.
Klarenbeek J, Goedhart J, Van Batenburg A, Groenewald D, Jalink K (2015). Fourth-generation Epac-based FRET sensors for cAMP feature exceptional brightness, photostability and dynamic range: Characterization of dedicated sensors for FLIM, for ratiometry and with high affinity. PLoS One 10, 1–11.
Kraakman L, Lemaire K, Ma P, Teunlssen A, Donaton MCV, Van Dijck P, Winderickx J, De Winde JH, Thevelein JM (1999). A Saccharomyces cerevisiae G-protein coupled receptor, Gpr1, is specifically required for glucose activation of the cAMP pathway during the transition to growth on glucose. Mol Microbiol 32, 1002–1012.
Lee REC, Walker SR, Savery K, Frank DA, Gaudet S (2014). Fold change of nuclear NF-κB determines TNF-induced transcription in single cells. Mol Cell 53, 867–879.
Lemaire K, Van De Velde S, Van Dijck P, Thevelein JM (2004). Glucose and sucrose act as agonist and mannose as antagonist ligands of the G protein-coupled receptor Gpr1 in the yeast Saccharomyces cerevisiae. Mol Cell 16, 293–299.
Lohr D, Venkov P, Zlatanova J (1995). Transcriptional regulation in the yeast GAL gene family: a complex genetic network. FASEB J 9, 777–787.
Ma P, Wera S, Van Dijck P, Thevelein JM (1999). The PDE1-encoded low-affinity phosphodiesterase in the yeast saccharomyces cerevisiae has a specific function in controlling agonist-induced cAMP signaling. Mol Biol Cell 10, 91–104.
Magherini F, Busti S, Gamberi T, Sacco E, Raugei G, Manao G, Ramponi G, Modesti A, Vanoni M (2006). In Saccharomyces cerevisiae an unbalanced level of tyrosine phosphorylation down-regulates the Ras/PKA pathway. Int J Biochem Cell Biol 38, 444–460.
Maier A, Völker B, Boles E, Fuhrmann GF (2002). Characterisation of glucose transport in Saccharomyces cerevisiae with plasma membrane vesicles (countertransport) and intact cells (initial uptake) with single Hxt1, Hxt2, Hxt3, Hxt4, Hxt6, Hxt7 or Gal2 transporters. FEMS Yeast Res 2, 539–550.
Martínez-Pastor MT, Marchler G, Schüller C, Marchler-Bauer A, Ruis H, Estruch F (1996). The Saccharomyces cerevisiae zinc finger proteins Msn2p and Msn4p are required for transcriptional induction through the stress response element (STRE). EMBO J 15, 2227–2235.
Mastop M, Bindels DS, Shaner NC, Postma M, Gadella TWJ, Goedhart J (2017). Characterization of a spectrally diverse set of fluorescent proteins as FRET acceptors for mTurquoise2. Sci Rep 7, 11999.
Mbonyi K, Beullens M, Detremerie K, Geerts L, Thevelein JM (1988). Requirement of one functional RAS gene and inability of an oncogenic ras variant to mediate the glucose-induced cyclic AMP signal in the yeast Saccharomyces cerevisiae. Mol Cell Biol 8, 3051–3057.
Munder T, Küntzel H (1989). Glucose-induced CAMP signaling in Saccharomyces cerevisiae is mediated by the CDC25 protein. Fed Eur Biochem Soc 242, 341–345.
Nikawa J, Sass P, Wigler M (1987). Cloning and characterization of the low-affinity cyclic AMP phosphodiesterase gene of Saccharomyces cerevisiae. Mol Cell Biol 7, 3629–3636.
Ozcan S, Johnston M (1995). Three different regulatory mechanisms enable yeast hexose transporter (HXT) genes to be induced by different levels of glucose. Mol Cell Biol 15, 1564–1572.
Pardo LA, Lazo PS, Ramos S (1993). Activation of adenylate cyclase in cdc25 mutants of Saccharomyces cerevisiae. FEBS Lett 319, 237–243.
Park JI, Grant CM, Dawes IW (2005). The high-affinity cAMP phosphodiesterase of Saccharomyces cerevisiae is the major determinant of cAMP levels in stationary phase: Involvement of different branches of the Ras-cyclic AMP pathway in stress responses. Biochem Biophys Res Commun 327, 311–319.
Paulo JA, O'Connell JD, Everley RA, O'Brien J, Gygi MA, Gygi SP (2016). Quantitative mass spectrometry-based multiplexing compares the abundance of 5000 S. cerevisiae proteins across 10 carbon sources. J Proteomics 148, 85–93.
Paulo JA, O'Connell JD, Gaun A, Gygi SP (2015). Proteome-wide quantitative multiplexed profiling of protein expression: Carbon-source dependency in Saccharomyces cerevisiae. Mol Biol Cell 26, 4063–4074.
Peeters K, *et al*. (2017). Fructose-1,6-bisphosphate couples glycolytic flux to activation of Ras. Nat Commun 8.
van der Krogt GNM, Ogink J, Ponsioen B, Jalink K (2008). A comparison of donor-acceptor pairs for genetically encoded FRET sensors: application to the Epac cAMP sensor as an example. PLoS One 3, e1916.
van der Plaat JB (1974). Cyclic 3',5'-adenosine monophosphate stimulates trehalose degradation in baker's yeast. Biochem Biophys Res Commun 56, 580–587.
van Heerden JH, Wortel MT, Bruggeman FJ, Heijnen JJ, Bollen YJM, Planqué R, Hulshof J, O'Toole TG, Wahl SA, Teusink B (2014). Lost in

transition: start-up of glycolysis yields subpopulations of nongrowing cells. Science 343, 1245114.
Pohlig G, Holzer H (1985). Phosphorylation and inactivation of yeast fructose-1,6- bisphosphatase by cyclic AMP-dependent protein kinase from yeast. J Biol Chem 260, 13818–13823.
Ponsioen B, Gloerich M, Ritsma L, Rehmann H, Bos JL, Jalink K (2009). Direct spatial control of Epac1 by cyclic AMP. Mol Cell Biol 29, 2521–2531.
Ponsioen B, Zhao J, Riedl J, Zwartkruis F, van der Krogt G, Zaccolo M, Moolenaar WH, Bos JL, Jalink K (2004). Detecting cAMP-induced Epac activation by fluorescence resonance energy transfer: Epac as a novel cAMP indicator. EMBO Rep 5, 1176–1180.
Reifenberger E, Boles E, Ciriacy M (1997). Kinetic characterization of individual hexose transporters of Saccharomyces cerevisiae and their relation to the triggering mechanisms of glucose repression. Eur J Biochem 245, 324–333.
Reijenga KA, Snoep JL, Diderich JA, van Verseveld HW, Westerhoff HV, Teusink B (2001). Control of glycolytic dynamics by hexose transport in Saccharomyces cerevisiae. Biophys J 80, 626–634.
Reinders A, Bürckert N, Boller T, Wiemken A, De Virgilio C (1998). Saccharomyces cerevisiae cAMP-dependent protein kinase controls entry into stationary phase through the Rim15p protein kinase. Genes Dev 12, 2943–2955.
Rødkaer SV, Faergeman NJ (2014). Glucose- and nitrogen sensing and regulatory mechanisms in Saccharomyces cerevisiae. FEMS Yeast Res 14, 683–696.
Rolland F, Wanke V, Cauwenberg L, Ma P, Boles E, Vanoni M, de Winde JH, Thevelein JM, Winderickx J (2001). The role of hexose transport and phosphorylation in cAMP signalling in the yeast Saccharomyces cerevisiae. FEMS Yeast Res 1, 33–45.
Rolland F, De Winde JH, Lemaire K, Boles E, Thevelein JM, Winderickx J (2000). Glucose-induced cAMP signalling in yeast requires both a G-protein coupled receptor system for extracellular glucose detection and a separable hexose kinase-dependent sensing process. Mol Microbiol 38, 348–358.
Rolland F, Winderickx J, Thevelein JM (2002). Glucose-sensing and -signalling mechanisms in yeast. FEMS Yeast Res 2, 183–201.
Ruan Y-L (2014). Sucrose metabolism: gateway to diverse carbon use and sugar signaling. Annu Rev Plant Biol 65, 33–67.
Russell M, Bradshaw-Rouse J, Markwardt D, Heideman W (1993). Changes in gene expression in the Ras/adenylate cyclase system of Saccharomyces cerevisiae: correlation with cAMP levels and growth arrest. Mol Biol Cell 4, 757–765.
Santangelo GM (2006). Glucose signaling in saccharomyces cerevisiae glucose signaling in Saccharomyces cerevisiae. Microbiol Mol Biol Rev 70, 253–282.
Smith A, Ward MP, Garrett S (1998). Yeast PKA represses Msn2p/Msn4p-dependent gene expression to regulate growth, stress response and glycogen accumulation. EMBO J 17, 3556–3564.
Stewart-Ornstein J, Chen S, Bhatnagar R, Weissman JS, El-Samad H (2017). Model-guided optogenetic study of PKA signaling in budding yeast. Mol Biol Cell 28, 221–227.
Takhaveev V, Heinemann M (2018). Metabolic heterogeneity in clonal microbial populations. Curr Opin Microbiol 45, 30–38.
Tanaka K, Matsumoto K, Toh-E A (1989). IRA1, an inhibitory regulator of the RAS-cyclic AMP pathway in Saccharomyces cerevisiae. Mol Cell Biol 9, 757–768.
Tanaka K, Nakafuku M, Tamanoi F, Kaziro Y, Matsumoto K, Toh-e A (1990). IRA2, a second gene of Saccharomyces cerevisiae that encodes a protein with a domain homologous to mammalian ras GTPase-activating protein. Mol Cell Biol 10, 4303–4313.
Thevelein JM (1991). Fermentable sugars and intracellular acidification as specific activators of the RAS-adenylate cyclase signalling pathway in yeast: the relationship to nutrient-induced cell cycle control. Mol Microbiol 5, 1301–1307.
Thevelein JM, Beullens M, Honshoven F, Hoebeeck G, Detremerie K, den Hollander JA, Jans AW (1987). Regulation of the cAMP level in the yeast Saccharomyces cerevisiae: intracellular pH and the effect of membrane depolarizing compounds. J Gen Microbiol 133, 2191–2196.
Toda T, Cameron S, Sass P, Zoller M, Scott JD, McMullen B, Hurwitz M, Krebs EG, Wigler M (1987). Cloning and characterization of BCY1, a locus encoding a regulatory subunit of the cyclic AMP-dependent protein kinase in Saccharomyces cerevisiae. Mol Cell Biol 7, 1371–1377.
Vanhalewyn M, Dumortier F, Debast G, Colombo S, Ma P, Winderickx J, Van Dijck P, Thevelein JM (1999). A mutation in Saccharomyces cerevisiae adenylate cyclase, Cyr1(K1876M), specifically affects glucose- and acidification-induced cAMP signalling and not the basal cAMP level. Mol Microbiol 33, 363–376.
Versele M, de Winde JH, Thevelein JM (1999). A novel regulator of G protein signalling in yeast, Rgs2, downregulates glucose-activation of the cAMP pathway through direct inhibition of Gpa2. EMBO J 18, 5577–5591.
Vidan S, Mitchell aP (1997). Stimulation of yeast meiotic gene expression by the glucose-repressible protein kinase Rim15p. Mol Cell Biol 17, 2688–2697.
Winderickx J, De Winde JH, Crauwels M, Hino A, Hohmann S, Van Dijck P, Thevelein JM (1996). Regulation of genes encoding subunits of the trehalose synthase complex in Saccharomyces cerevisiae: Novel variations of STRE-mediated transcription control? Mol Gen Genet 252, 470–482.
Xiao Y, Bowen CH, Liu D, Zhang F (2016). Exploiting nongenetic cell-to-cell variation for enhanced biosynthesis. Nat Chem Biol 12, 339–344.
Xu Z, Tsurugi K (2006). A potential mechanism of energy-metabolism oscillation in an aerobic chemostat culture of the yeast Saccharomyces cerevisiae. FEBS J 273, 1696–1709.
Youk H, van Oudenaarden A (2009). Growth landscape formed by perception and import of glucose in yeast. Nature 462, 875–879.
Yun C, Tamaki H, Nakayama R, Yamamoto K, Kumagai H (1998). Gpr1p, a putative G-protein coupled receptor, regulates glucose-dependent cellular cAMP level in Yeast Saccharomyces cerevisiae. Biochem Biophys Res Commun 252, 29–33.